WELDING RESEARCH

SUPPLEMENT TO THE *WELDING JOURNAL,* OCTOBER 2014
Sponsored by the American Welding Society and the Welding Research Council

Mechanical Behavior of Titanium-Clad Steel Welded Joints

Mechanical properties of Ti-clad steel welded joints deposited with different interlayer materials were evaluated using microhardness, bend, and shear-bond strength testing in the as-welded, after PWHT, and in thermally cycled conditions.

BY J. E. RAMIREZ

ABSTRACT

Ti-clad steel welded joints made with different interlayer material-joining process combinations were evaluated using microhardness, bend, and shear-bond strength testing. The effect of thermal cycling on the shear-bond strength was evaluated as well. In general, all the welded joints present the highest hardness level at the interlayer-Ti interface and across the first Ti layer. The maximum hardness in welded joints made with the Ni-Ti, NiCu-Ti, and NiCr-Ti interlayer systems was 607, 568, and 554 $HV_{0.5}$, respectively. In the V-Ti and Ti-V systems, the respective maximum hardnesses were 307 and 409 $HV_{0.5}$, respectively, at the Fe-V interface. The maximum hardness observed in welded joints made with the Cu-Ti interlayer ranged from 300 to 350 $HV_{0.5}$. Different softening responses to either thermal cycles of additional Ti layers or PWHT were observed in different types of joints. Most of the joints failed the bend tests in the as-welded and PWHTed conditions. The Ni-Ti-, NiCu-Ti-, and NiCr-Ti-welded joints failed along the interlayer-Ti interface and through the Ti weld layers. The Cu-Ti welded joints made with the CSC-GMAW process failed along the Cu-Ti interface. The bond-shear strength of both Fe-Cu and Cu-Ti interfaces in Cu-Ti welded joints made with a combination of CSC-GMAW and GTAW-P processes in the as-welded, PWHTed, and thermally cycled conditions ranged from 204.5 to 259.8 MPa (29.6 to 37.6 ksi). The Fe-Cu interface showed a larger displacement under maximum load as compared to that observed in the Cu-Ti interface.

KEYWORDS

• Cladding • Titanium • Ti-Clad Steel • Thermal Cycling • Interlayer Materials

Introduction

Titanium (Ti) clad steel is widely used for large pressure vessels and other equipment in different industries to take advantage of the corrosion resistance of Ti, but at a lower cost than solid Ti construction. Titanium-clad steel is produced by roll bonding (usually with an interlayer), direct explosive bonding (usually without an interlayer) (Ref. 1), or by a combination of explosive bonding and roll bonding (Ref. 2). Interlayers are used to improve the bond strength of the clad steel or to overcome metal plasticity compatibility restrictions encountered in roll bonding. Industrial-grade pure iron (Fe), ultralow-carbon steel, niobium (Nb) alloys, tantalum (Ta) alloys, copper (Cu) alloys, and nickel (Ni) alloys have been used as interlayers in the cladding process (Refs. 3–6). Typical thickness of Ti-clad ranges from 2.0 to 19.0 mm (0.08 to 0.75 in.) depending on the application.

Titanium has not been successfully fusion welded directly to steel because it has limited solubility for Fe. If the solubility limit is exceeded, as in fusion welding, brittle intermetallic compounds and carbides form (Refs. 7, 8). Cracks form in these phases due to the thermal stresses induced during cooling and complete separation along the Fe-Ti interface may happen in the welded joint, as shown in Fig. 1. To avoid welding Ti directly to steel, the most common method of joining clad plates is the Batten Strip technique (Refs. 1, 9–11). The Ti cladding material is stripped back 15 to 20 mm from the weld joint, after which the steel is welded and inspected. Next, the space where the cladding was removed is filled with Cu, Ti, or steel filler strips. Finally, a Ti cover strip or Batten Strip about 50mm wide is welded over the joint using fillet welds and gas tungsten arc welding (GTAW) techniques. This method has several disadvantages including complexity of irregular geometry at nozzle penetrations and attachments, complexity of testing for joint integrity (including no reliable method to inspect for root side purge failure), open root joint configuration subject to widespread corrosion damage of the steel in the event of local failures of the fillet welds on the batten strips, potential for service failures due to low-cycle fatigue, difficulty of repair, and relatively high fabrication and testing costs.

Therefore, there is the need to develop reliable cost-effective methods of joining or repairing Ti-clad steel

J. E. Ramirez (jose.ramirez@dnvgl.com) *was a principal engineer with EWI and now is a principal engineer at DNV.GL in Columbus, Ohio.*

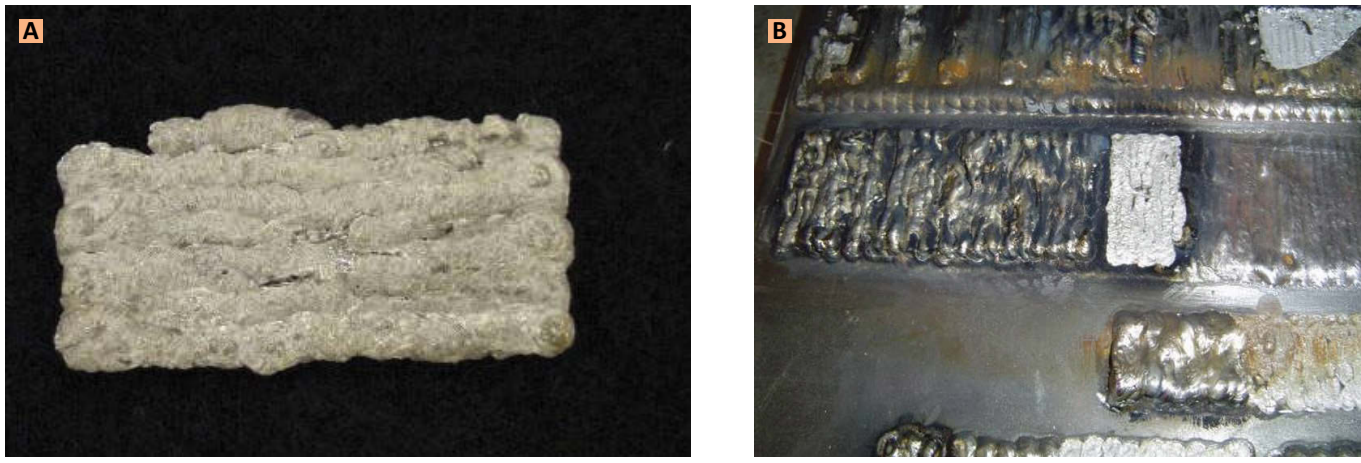

Fig. 1 — A — Titanium deposit layer that cracked and broke off a commercially pure Fe weld deposit during cooling; B — weld deposit that cracked.

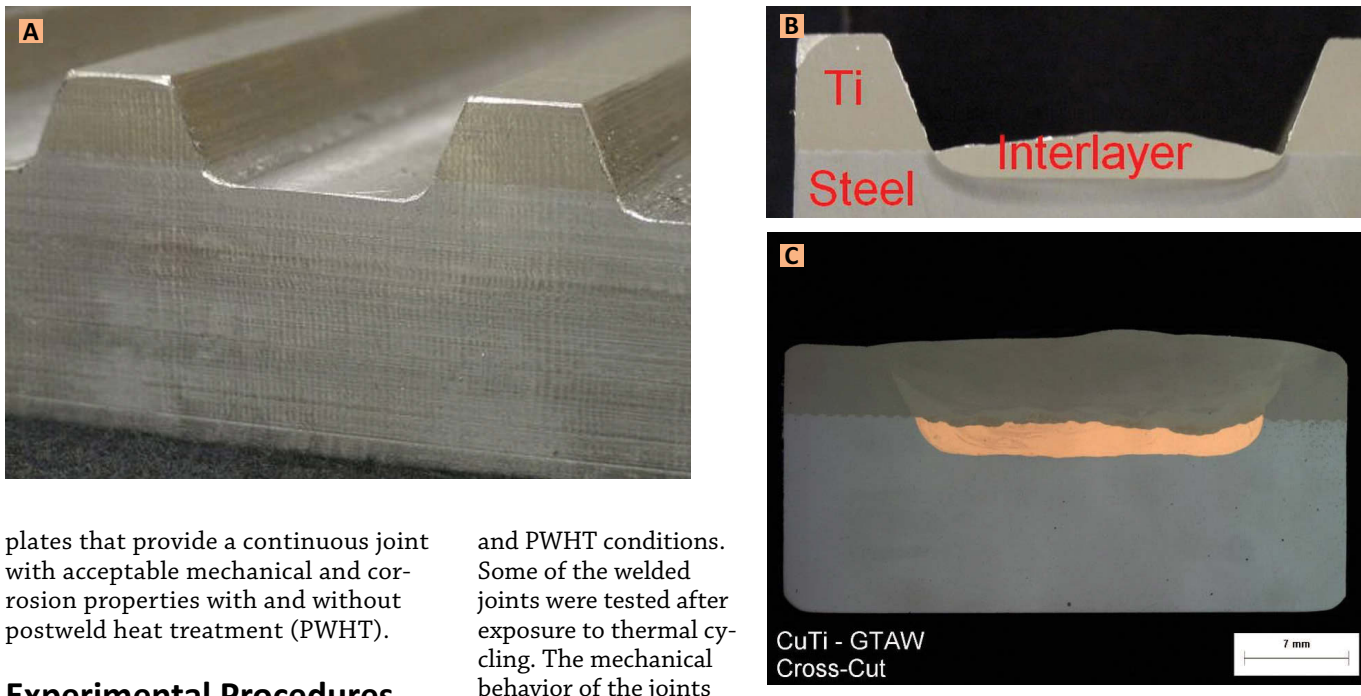

Fig. 2 — A — General view of joint design; B — cross section of joint after deposition of interlayer material; C — after completion of the joint.

plates that provide a continuous joint with acceptable mechanical and corrosion properties with and without postweld heat treatment (PWHT).

Experimental Procedures

Ti-clad steel welded joints were made using different interlayer material-joining process combinations. The welded joints were tested in as-welded and PWHT conditions. Some of the welded joints were tested after exposure to thermal cycling. The mechanical behavior of the joints was evaluated using microhardness, bend, and shear bond strength testing.

Table 1 — General Characteristics of the Welding Consumables Used as Interlayer Materials and Ti Layer for Welding the Ti-Clad Steel Plates

Joint Designation	Welding Process	Filler Metal Designation	Wire Size (in.)
Ni-Ti	CSC-GMAW	CPNi (ERNi-1)	0.062
NiCu-Ti	CSC-GMAW	NiCu (ERNiCu-7)	0.062
NiCr-Ti	CSC-GMAW	NiCr (ERNiCr-4)	0.062
Cu-Ti	CSC-GMAW	CPCu (ERCu)	0.062
Cu-Ti	CSC-GMAW	CPCu (ERCu)	0.062
	GTAW	CPTi (ERTi-1)	0.035
V-Ti	GTAW	—	0.062/0.045
Ti Layers	CSC-GMAW/GTAW	ERTi-1	0.062/0.035

Materials and Welding Conditions

Titanium-Clad Base Metal and Interlayer Materials

The deposition of the interlayer material and corresponding Ti layers of the welded joints was done in 150- × 200-mm (6- × 8-in.) explosion Ti-clad steel samples. The explosion Ti-clad steel base metals consisted of SA-516-70 carbon steel with a nominal thickness of 27.5 to 38.0 mm (1.1 to

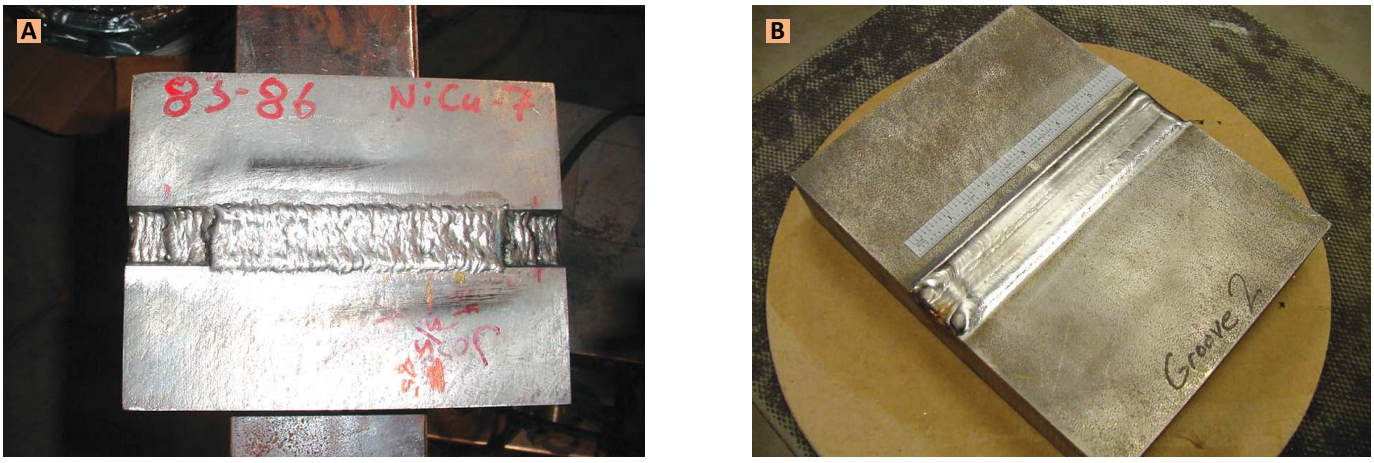

Fig. 3 — A — General view of Ti-clad steel welded joints made with the CSC-GMAW process; B — joint made with a combination of the CSC-GMAW and the GTAW-P processes.

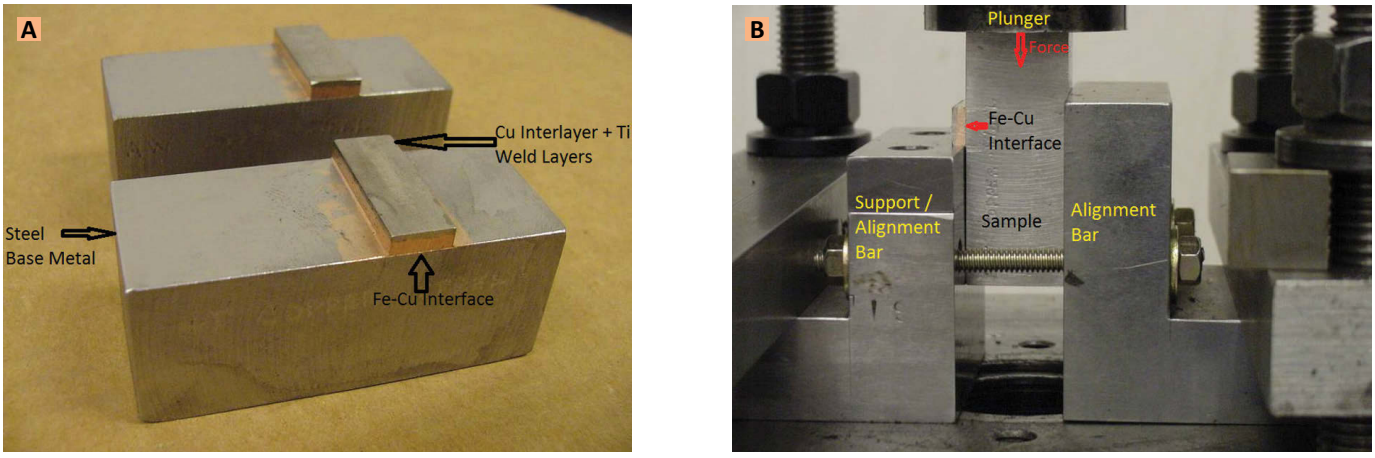

Fig. 4 — A — General view of Fe-Cu interface bond shear-strength samples; B — test setup.

1.5 in.) and SB-265-1 Ti clad with a nominal thickness between 4.8 to 8.0 mm (0.188 to 0.313 in.). Based on metallurgical characteristics and potential compatibility with the Fe-Ti system, and availability as commercial welding wires, the interlayer materials that were used for joining Ti-clad steel include commercially pure (CP) nickel (Ni), nickel-copper alloy (NiCu), nickel-chromium alloy (NiCr), CP vanadium (V), and CP copper (Cu) (Ref. 12). The general description of the welding consumables used for welding of the Ti-clad steel plates is listed in Table 1.

Joint Design

The Ti-clad steel base metal samples have a widegroove prepared by the strip-back method. The joint design of the wide-groove included a root that was between 19.0 to 25.0 mm

Table 2 — Ranking in Decreasing Order of Suitability of Interlayer-Welding Process Combination for Making Full-Size Ti-Clad Steel Welded Joints

Ranking	Description of Interlayer System: Interlayer Design [a]	Welding Process	Comments
1	Fe-Cu-Ti	CSC-GMAW + GTAW-P	1. Poor wettability of Ti on Cu
2	Fe-Cu-Ti	CSC-GMAW	1. Short contact tip life during deposition of Ti 2. Poor wettability of Ti on Cu
3	Fe-Ni-Ti	CSC-GMAW	1. Short contact tip life during deposition of Ti 2. Cracking susceptibility
4	Fe-NiCu-Ti	CSC-GMAW	1. Short contact tip life during deposition of Ti 2. Cracking susceptibility
5	Ti-V-Fe	GTAW-P	1. Cracking susceptibility
6	Fe-NiCr-Ti	CSC-GMAW	1. Short contact tip life during deposition of Ti 2. Cracking susceptibility

(a) The designation of the interlayer system indicates the sequence of deposition of the different interlayer materials and Ti layers in the joint.

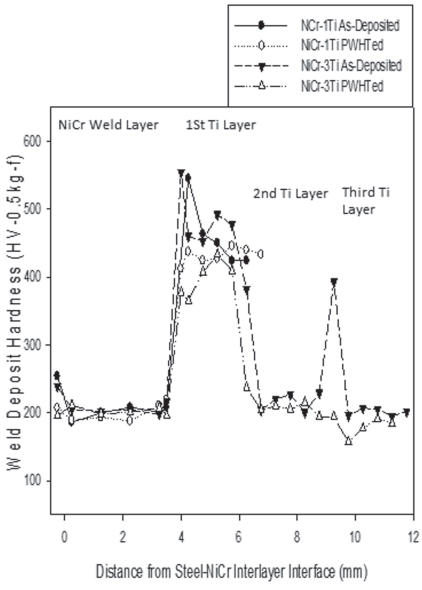

Fig. 5 — Microhardness profile of NiCr-Ti welded joint with one and three Ti weld metal layers (1Ti, 3Ti), in the as-welded and PWHTed conditions (CSC-GMAW process).

(0.75 to 1.0 in.) wide and a 22-deg bevel angle. Additionally, the groove was machined to a depth of about 2.50 mm (0.10 in.) into the steel substrate, as shown in Fig. 2A and B. This joint design replicates the Ti portion of Ti-clad steel butt joints, which is the more critical part of this type of joint.

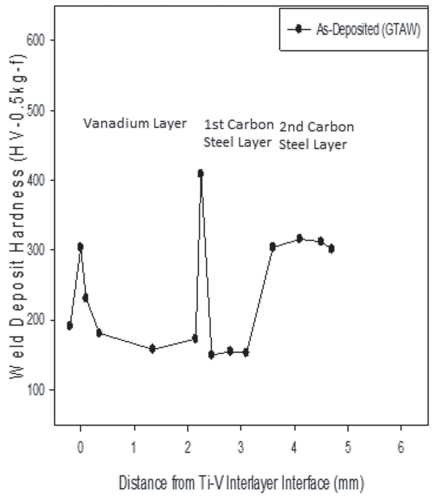

Fig. 6 — Microhardness profile of Ti-V-Fe welded joint with two carbon-steel weld metal layers, in the as-welded condition (GTAW-P process).

Welding Process

Different joining processes were considered based on the metallurgical characteristics of the selected interlayers, and on the typical dilution of the joining processes. The latter is significant because low-dilution processes limit the amount of melting, as well as the thermal experience of the base metal at temperatures where intermetallic compounds may form. Considering the commercial availability of consumables, ease of deployment in the field, and relatively low equipment investment, arc welding processes were considered the primary process of choice.

A relatively new gas metal arc welding (GMAW) process variant called controlled short circuit (CSC)-GMAW was chosen to deposit the selected interlayers and Ti layers in the welded joints. The CSC-GMAW process involves "pulsing" the wire feed in conjunction with the welding current to achieve improved control of welding heat input and dilution with minimal spatter. Welding parameters of the CSC-GMAW process include up-wire feed speed (Up WFS) (m/min), down-WFS (m/min), initial arc length (mm), arc current sequence, and short-circuit current sequence. Each current sequence has three levels to set (start, pulse, and end). These three cur-

Table 3 — Welding Conditions for Depositions of Different Layers of Weld Metal in the Weld Joints Using CSC-GMAW

		Arc Current Sequence					Short-Circuit Current Sequence				
Weld Layer	Shielding Gas	Start Current (A)	Start Current Time (ms)	Pulse Current (A)	Pulse Current Time (ms)	End Current (A)	Start Current (A)	Start Current Time (ms)	Pulse Current (A)	Pulse Current Time (ms)	End Current (A)
Ni on steel	100% He	100	NA	100	NA	100	50	NA	50	NA	50
Ti on Ni	100% He	80	5	60	5	40	40	2.5	60	NA	60
NiCu on steel	100% He	100	NA	100	NA	100	50	NA	50	NA	50
Ti on NiCu	100% He	80	5	60	5	40	40	2.5	60	NA	60
NiCr on steel	50%Ar/50%He	100	NA	100	NA	100	50	NA	50	NA	50
Ti on NiCr	100% He	80	5	60	5	40	40	2.5	60	NA	60
CPCu on steel	100% He	130	NA	130	NA	130	50	NA	50	NA	50
CPCu on steel	100% He	150	NA	150	NA	150	50	NA	50	NA	50
Ti on CpCu	100% He	120	5	100	5	80	40	2.5	60	NA	60
Ti on Ti	100% He	80	5	60	5	40	40	2.5	60	NA	60

Wire Feed Speed		Initial Arc Length (mm)	Weaving Parameters			
Up WFS (m/min)	Down WFS (m/min)		Oscillation Speed (mm/s)	Dwell Time(s)	Oscillation Amplitude (mm)	Forward Travel Speed (mm/s)
10	15	0.0	7.4	0.2	19.8	27.6
8	10	1.0	12.0	0.3	22.9	11.8
10	15	0.0	9.4	0.2	20.3	27.6
8	10	0.5	12.0	0.3	23.6	11.8
15	15	0.0	7.4	0.2	21.1	31.5
8	10	0.5	12.0	0.3	22.3	11.8
15	15	0.0	14.6	0.3	17.8	11.0
10	10	0.0	19.8	0.3	16.5	11.0
8	10	0.0	12.0	0.3	21.1	11.8
8	10	0.5	12.0	0.3	23.6	11.8

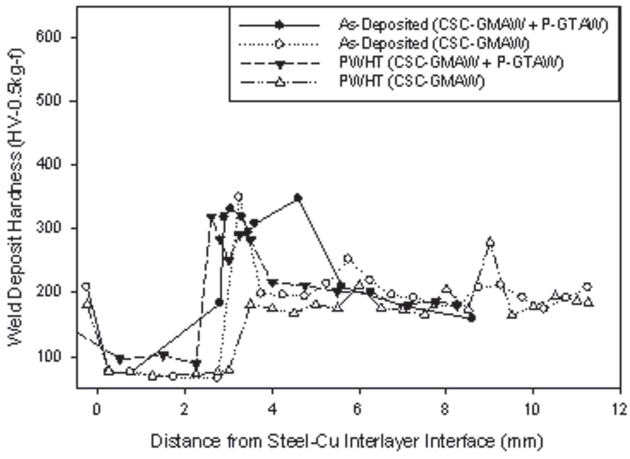

Fig. 7 — Comparison of microhardness profiles of Cu-Ti welded joints with three Ti weld metal layers deposited with the CSC-GMAW process and with a combination of CSC-GMAW and GTAW-P processes.

Fig. 8 — General view of side bend samples obtained from NiCu-Ti welded joints in the as-welded and PWHT conditions (CSC-GMAW process).

rent levels are used to control the bead shape and size. The start and pulse levels have a time associated with them. For the end current level, the current is maintained until the next sequence is initiated.

During the arc phase, the end of the electrode is melted and a droplet is formed. At the same time, the electrode is feeding forward toward the weld pool. The forward wire feeding speed is set higher than the melt-off rate so that the arc will short out. Upon shorting, the droplet at the end of the electrode is pulled into the weld pool by the liquid pool's surface tension. The control system senses the voltage drop and prevents the current from spiking severely. A current sequence is implemented to allow resistive heating. The heat allows for a smooth arc ignition. At the same time, the wire feeders reverse direction so that the electrode is being pulled away from the weld pool. This makes the short circuit break mechanically. This differs from any other short-circuiting process, which relies on the electrode exploding to reestablish the arc. The process represents an advance in short-circuit metal transfer of the GMAW process (Refs. 13–17) and offers reduced heat input and dilution compared to other arc welding processes.

Welding Conditions

Due to the complexity inherent to dissimilar metal joining, CSC-GMAW welding parameters and weaving parameters were developed and optimized (Ref. 18). Six interlayer-joining process combinations were ranked based on their general wettability behavior, weldability, and the ability to achieve acceptable welding conditions, as listed in Table 2. Table 3 lists the CSC-GMAW welding parameters developed and used for depositing each interlayer material and the subsequent Ti layers in the welded joints. The GTAW-P parameters used to deposit the different Ti layers in welded joints made with the Cu-Ti interlayer system are listed in Tables 4–6.

Figure 3 shows a general view of some of the welded joints made for mechanical evaluation. The welded joint in Fig. 3A shows a stepwise configuration at the ends. The three levels of the stepwise configuration from the end toward the center of the sample correspond to the surface of the weld deposit of the interlayer material, the surface of the first Ti deposit layer, and the surface of two additional layers of Ti. This arrangement allowed the characterization of deposits of the interlayer material in the as-welded condition and an evaluation of the effects of thermal cycles induced during the deposition of one and three layers of Ti on the properties of the interlayer materials and the welded joint as a whole. Figure 2C shows a cross section of a complete welded joint (interlayer material plus three Ti layers). The welded joints were subjected to radiographic examination to evaluate the soundness of the joints and to determine the location of different specimens required for the mechanical evaluation.

Postweld Heat Treatment

The PWHT of the welded joints was conducted following the guidelines of Section VIII of the ASME code for carbon steel welded constructions. The holding temperature was between 1125° and 1150°F (607° and 620°C) and the holding time ranged from 1 h, 15 min. to 1 h, 52 min. depending on the thickness of the full-size joint. Heating rates above 800°F (427°C)

Table 4 — GTAW-P Parameters Used for the Deposition of First Layer of Ti in the Cu-Ti welded Joint

Peak current (A)	250	Wire feed peak (mm/s)	8.5
Back current (A)	10	Wire feed back (mm/s)	8.0
Peak current time (s)	0.1	Arc voltage (V)	12.2
Back current time (s)	0.5	Travel speed (mm/s)	1.1
Wire entry angle (deg)	15	Wire to electrode distance (mm)	1.1
Wire type	ERTi-1	Wire diameter (mm)	0.9
Electrode type	2% Ce	Electrode diameter (mm)	3.2
Electrode preparation (deg)	30, no flat	Shielding gas type	75% He 25% Ar

Fig. 9 — Cracks observed in longitudinal side bend samples obtained from Ti-V-Fe welded joints in the PWHT condition (GTAW-P process).

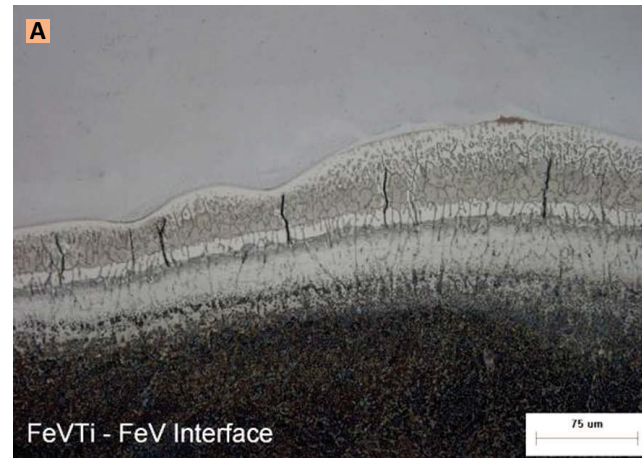

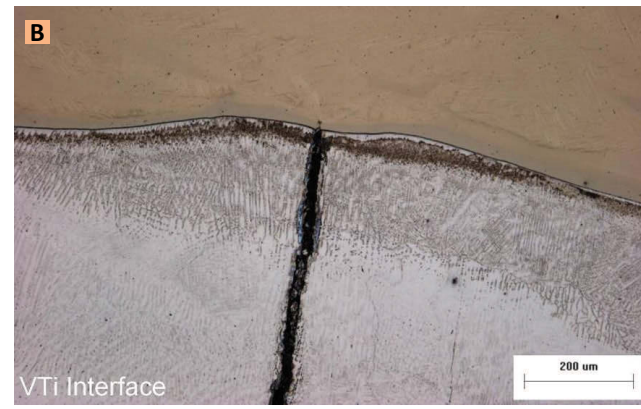

Fig. 10 — A — Microcracking observed in the Fe-V interface of welded joints deposited with the GTAW-P process; B — crack arrested at the V-Ti interface.

were controlled to be equal or less than 400°F/h/in. (8.7°C/h/mm). Cooling rates above 800°F (427°C) were equal or less than 500°F/h/in. (10.9°C/h/mm).

Evaluation of Mechanical Behavior of Welded Joints

The Ti-clad steel welded joints were evaluated before and after PWHT. The joints were evaluated using microhardness profiles, bend testing, and bond shear-strength testing. The effect of thermal cycling after PWHT on the shear-bond strength of some joints was evaluated as well.

Microhardness Testing

Microhardness profiles were determined in the through-thickness direction of the deposited weld metals starting from the steel substrate toward the surface of the last layer of Ti weld deposit. The microhardness profiles of the welded joints were determined in deposits with one and three Ti layers, respectively, and in the as-welded and PWHT conditions. The hardness reading was determined using hardness Vickers scale with a load of 500 g ($HV_{0.5}$).

Bend Testing

The ductility of the welded joints was evaluated using transverse and longitudinal side-bend tests of samples in the as-welded and PWHT conditions. Two samples in the as-welded condition and two samples in the PWHT condition from each system were tested for a total of four specimens per welded joint. According to the requirements of the ASME code Section IX, the bend tests were run using an 8T diameter mandrel or die, where T is the thickness of the bend sample.

Bend testing was not conducted in welds made with the Fe-V-Ti interlayer system because crack-free joints were difficult to make. Additionally, welded joints from the Ti-V-Fe system were tested only in the PWHT conditions because the bend samples cracked during machining in the as-welded conditions. This may indicate the buildup of a high level of residual stresses during the welding of this dissimilar metal joint.

Table 5 — GTAW-P Parameters Used for the Deposition of Second Layer of Ti in the Cu-Ti

Peak current (A)	160	Wire feed peak (mm/s)	6.4
Back current (A)	80	Wire feed back (mm/s)	6.4
Peak current time (s)	0.1	Arc voltage (V)	9.2
Back current time (s)	0.25	Travel speed (mm/s)	1.1
Wire entry angle (deg)	15	Wire to electrode distance (mm)	1.1
Wire type	ERTi-1	Wire diameter (mm)	0.9
Electrode type	2% Ce	Electrode diameter (mm)	3.2
Electrode preparation (deg)	30, no flat	Shielding gas type	75% He 25% Ar

Bond Shear-Strength Testing

In order to measure the shear bond strength of interfaces between dissimilar material layers in some of the welded joints, shear-strength testing was conducted according to the requirements of ASTM B898 (Ref. 19). Figure 4 shows a view of some Fe-Cu interface shear bond strength samples, and test setup. As shown in Fig. 4B, the sample is set between two alignment bars to control lateral displacement of the sample and force the sample to move only in the vertical direction. One of the alignment bars also acts as support (left-side bar in

Fig. 11 — General view of side bend samples obtained from Cu-Ti welded joints in the as-welded and PWHT conditions (CSC-GMAW process).

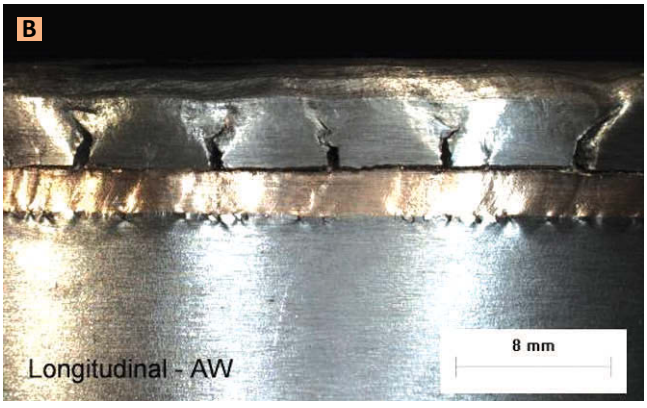

Fig. 12 — A — General view of bend test samples; B — cracks observed in longitudinal side bend. Samples obtained from Cu-Ti welded joints in the as-welded and PWHT conditions (combination of CSC-GMAW and GTAW-P processes).

Fig. 4B) to restrict the vertical displacement of the area of the sample corresponding to the interlayer material and/or Ti weld layers. The rest of the sample can be displaced freely in the vertical direction. During testing, loading was applied to the sample in the vertical-down direction through a plunger, as shown in Fig. 4B. As a result of the plunger force and restraint of the alignment/support bar, a shear force was induced at the interface under evaluation. Only welded joints made with the Cu-Ti interlayer system using a combination of CSC-GMAW and GTAW-P processes were tested. The shear bond strength of the Fe-Cu and Cu-Ti interfaces was determined in the as-welded and in the PWHT condition.

Effect of Thermal Cycling

A section from a welded joint made with the Ti-Cu/(CSC-GMAW + GTAW-P) combination and in the PWHT condition was subjected to 12 thermal cycles. During each thermal cycle, the sample was heated to a temperature of 496°C ±14° (925°F ±25°) and held at that temperature for one hour. The sample was then allowed to cool to a temperature less than 38°C (100°F). The sample was visually inspected and evaluated with dye penetrant before and after the 12 thermal cycles were completed to determine the presence of cracks. No cracking was observed in the sample. Based on these results, one shear bond strength coupon representing the Fe-Cu interface and a shear bond strength coupon representing the Cu-Ti interface was machined and tested according to the requirements of ASTM B898. The shear bond strength results were compared to those obtained from specimens that were not exposed to thermal cycling.

Experimental Observations and Discussions

Microhardness Profiles

Microhardness profiles obtained from some of the welded joints are shown in Figs. 5–7. In general, all the welded joints present the highest hardness level at the interlayer-Ti interface and across the first Ti layer, as can be observed in Fig. 5. This is consistent with the results of the light- and electron-microscopy characterizations of the weld metal deposits that indicated the presence of second phases in those regions of the welded joints, as reported in a previous paper (Ref. 12). The maximum hardnesses in the welded joints made with the Ni-Ti, NiCu-Ti, and NiCr-Ti interlayer systems were 607, 568, and 554 $HV_{0.5}$, respectively. In the V-Ti and Ti-V systems, the maximum hardness readings obtained from the weld deposits

Table 6 — GTAW-P Parameters Used for the Deposition of Filling Layers of Ti in the Cu-Ti Welded Joint

Peak current (A)	140	Wire feed peak (mm/s)	10.6
Back current (A)	140	Wire feed back (mm/s)	10.6
Peak current time (s)	0.1	Arc voltage (V)	9.5
Back current time (s)	0.25	Travel speed (mm/s)	1.5
Wire entry angle (deg)	15	Wire to electrode distance (mm)	1.1
Wire type	ERTi-1	Wire diameter (mm)	0.9
Electrode type	2% Ce	Electrode Diameter (mm)	3.2
Electrode preparation (deg)	30, no flat	Shielding gas type	75% He 25% Ar

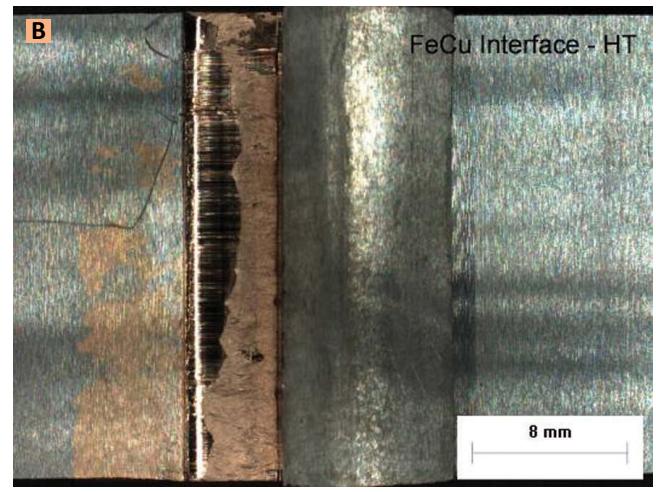

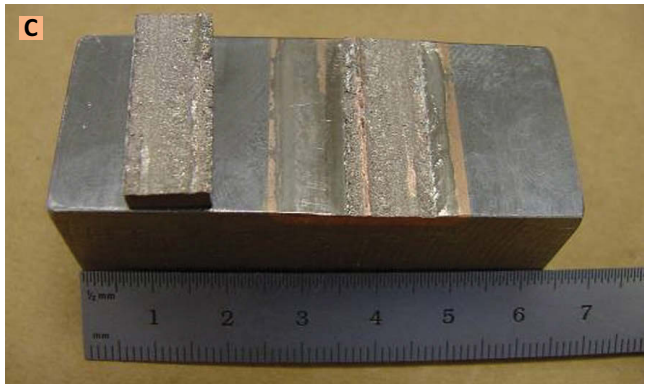

Fig. 13 — A — General view of bond shear strength samples of the Fe-Cu and Cu-Ti interfaces; B — ductile characteristics of the shear fracture of the Fe-Cu interface; C — brittle characteristics of the shear fracture of the Cu-Ti interface.

were 307 and 409 $HV_{0.5}$, respectively, at the Fe-V interface. The maximum hardnesses observed in the welded joints made with the Cu-Ti interlayer ranged from 300 to 350 $HV_{0.5}$.

Different softening responses to thermal cycles induced by either welding of additional layers of Ti weld metal or PWHT were observed in different welded joints. In the Ni-Ti welded joints, more softening was induced in the interface and first layer of Ti weld deposit by deposition of additional layers of Ti weld metal than that induced by the PWHT. The hardness of the NiCr-Ti welded joint with three Ti-layers shows a high value near the interface between the second and third Ti layers, as shown in Fig. 5, but the interface softened as a result of the PWHT. In general, the NiCu-Ti and NiCr-Ti welded joints did not experience major softening as a result of the thermal experience induced during either welding or PWHT, as shown in Fig. 5.

In the Fe-V-Ti system, extremely high hardness was not observed across the weld deposit, in spite of the observed presence of second phases at the Fe-V interface (Ref. 12). However, the presence of microcracks at the Fe-V interface may have influenced the results of the hardness readings. On the other hand, in the Ti-V-Fe system, a high hardness peak was observed at the V-Fe interface, as shown in Fig. 6. This may have resulted from a potential combination of Fe and Ti at that interface. The high degree of solid solubility between V and Ti could have induced a relatively high concentration of Ti in the V weld deposit, making it available for reaction with Fe at the V-Fe interface. Electron probe microanalyzer (EPMA) analysis was not conducted in weld metal deposits made with either the Fe-V-Ti system or the Ti-V-Fe system to confirm this statement. The weld metal of the Cu-Ti welded joints shows the softest deposits, especially in the PWHT condition. This system experiences more softening during PWHT than during additional welding thermal cycles. In the Cu-Ti system, as a result of the PWHT, the hardness level through the weld deposit dropped to around 200 $HV_{0.5}$. Due to a wider Cu-Ti interface in weld metal deposited with a combination of CSC-GMAW and GTAW-P processes (as compared to that deposited with only the CSC-GMAW process), a wider hard region at the Cu-Ti interface and a lower degree of softening induced by the PWHT were observed, as shown in Fig. 7.

Table 7 — Bond Shear Strength of the Fe-Cu and Cu-Ti Interfaces in Ti-Clad Steel Welded Joint Deposited with a Combination of CSC-GMAW and GTAW-P Processes, in the As-Welded, PWHTed, and Thermal Cycled Conditions

Interface	Condition	Bond Shear Strength MPa (ksi)
Fe-Cu	As-welded	204.5 (29.6)
	PWHTed	222.6 (32.2)
	Thermal cycled	230.0 (33.3)
Cu-Ti	As-welded	259.8 (37.6)
	PWHTed	227.2 (32.9)
	Thermal cycled	231.9 (33.6)
ASTM B898-99 Requirements		137.9 (20.0)

Side Bend Tests

Most of the bend samples obtained from the welded joints failed the bend test in the as-welded and PWHT conditions. Bend samples from the Ni-Ti, NiCu-Ti, and NiCr-Ti welded joints failed primarily along the interlayer-Ti interface and through the Ti weld deposits, as shown in Fig. 8. This may be due to the formation of a wide and continuous hard interlayer-Ti interface consisting of second phases, as well as

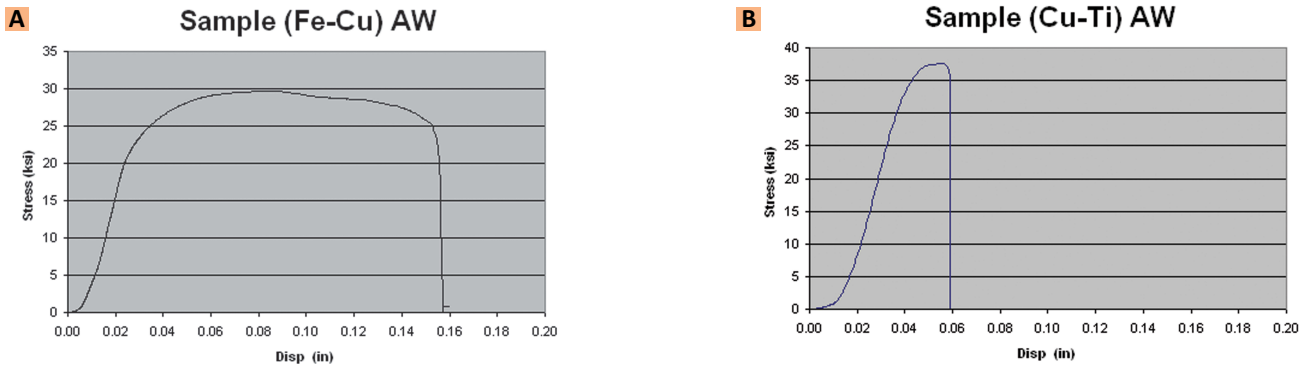

Fig. 14 — A — Stress-displacement curve obtained during the bond shear strength testing of the Fe-Cu interface; B — Cu-Ti interface from welded joint in the as-welded conditions (combination of CSC-GMAW and GTAW-P processes).

the presence of second phases through the first Ti layer (Ref. 12). In the NiCr-Ti interlayer system, second phases were observed even in the third layer of Ti weld deposits (Ref. 12). The distribution of these hard, low-ductility phases through the weld deposits may determine the paths of the cracks observed in the tested specimens.

As shown in Fig. 9, a bend sample obtained from a Ti-V-Fe welded joint in the PWHT condition showed the presence of small cracks in the sample; however, the cracks were perpendicular to the Ti-V and V-Fe interfaces and were confined to the V layer. This behavior may be due to the microstructural characteristics and mechanical properties of these two interfaces. The Ti-V interface was mainly free of second phase precipitation, and was narrow and well defined (Ref. 12). The presence of microcracking in the V-Fe interface after welding, as shown in Fig. 10A, may have acted as the nucleation sites for the cracks induced during the bend test. The good ductility of the steel weld metal deposits and of the Ti-V interfaces may have arrested the cracks, as shown in Fig. 10B.

The criteria established in the ASME code Section IX for the evaluation of a bend test as part of qualification of a welding procedure indicate that no crack larger than 3.0 mm (⅛ in.) in any direction is allowed. However, in this specific case, the thickness of the V layer was less than 3.0 mm (⅛ in.). As a result, all the cracks observed in the bend sample were shorter than 3.0 mm (⅛ in.). Therefore, this bend sample met the requirements established by the ASME code. Additionally, the amount of strain imposed during the bend test is larger than that imposed by most metalworking processes used during the manufacturing of a vessel or during service. However, questions arise regarding the unknown behavior of these microcracks that may be present at the Fe-V interface during service and their potential effect on the integrity of a vessel.

Most of the bend samples obtained from Cu-Ti welded joints made with the CSC-GMAW process failed along the Cu-Ti interface, as shown in Fig. 11. This behavior may be due to the narrow Cu-Ti interface, and the low degree of alloying of Cu in the Ti weld metal deposits observed in these welded joints (Ref. 12). Cracking was not observed in any one of the three layers of Ti weld deposits. Low dilution of the Ti weld metal may be responsible for the good ductility of the Ti weld deposit observed during the bend test.

Conversely, the transverse and longitudinal bend samples obtained from Cu-Ti welded joints made with a combination of CSC-GMAW and GTAW-P processes showed the presence of cracking along the Cu-Ti interface and cracks in the first Ti layer that were perpendicular to this interface, as shown in Fig. 12. This different behavior (compared to the welds made only with the CSC-GMAW process) may have resulted from a wider hard Cu-Ti interface observed in the welded joints made with a combination of welding processes. The cracking did not propagate through the complete thickness of the Ti-weld deposits, which indicates a good ductility of the last two layers of Ti weld deposited in the welded joints.

Bond Shear Strength and Effect of Thermal Cycling

The results of the bond shear strength testing of the Fe-Cu and Cu-Ti interfaces in Cu-Ti welded joints made with a combination of CSC-GMAW and GTAW-P processes in the as-welded, PWHT, and thermal-cycled conditions are listed in Table 7. The bond shear strength of both interfaces in all conditions ranged from 204.5 to 259.8 MPa (29.6–37.6 ksi) and is higher than the requirement of 137.9 MPa (20.0 ksi) established by standard ASTM B898-99. The shear bond strength of both interfaces was not affected by thermal cycling.

As shown in Fig. 13A and B, the Fe-Cu interface did not experience complete separation during testing. The shear path was located only along the Cu weld metal deposit. This may have resulted from the large difference in strength between the carbon steel substrate and the Cu deposit as indicated by the microhardness profile shown in Fig. 7. The small tolerances allowed in the testing setup may have also contributed to this behavior. Figure 13B shows the ductile characteristics of the shear fracture of the Fe-Cu interface.

Conversely, the Cu-Ti interface in the as-welded and PWHT conditions separated completely during the test, as shown in Fig. 13A and C. The shear path was located along the Cu-Ti interface. Although there is also a large difference in strength between the Cu deposit and the first Ti layer as shown in Fig. 7, the configuration of the test setup forced the fracture to take place along the interface or along the first Ti layer. Figure 13C shows the brittle characteristics of

the shear fracture of the Cu-Ti interface; however, in the thermal-cycled condition, the Cu-Ti interface did not experience complete separation.

The strength-displacement curves obtained during the bond shear tests also indicate the more ductile behavior of the Fe-Cu interface as compared to the behavior observed in the Ti-Cu interface. The Fe-Cu interface shows a larger displacement under maximum load as compared to that observed in the Cu-Ti interface, as shown in Fig. 14.

Based on the experimental observations, the multilayer approach used in the Ti-clad steel welded joints resulted in great improvement in mechanical behavior of the welded joints. Even though none of the weld joints passed the bend test, the multilayer approach resulted in an improved ductility as compare to the high degree of embrittlement normally observed in welds joining Ti directly to steel, as shown in Fig. 1. Therefore, it is recommended that the multilayer approach be further explored as a way to develop reliable cost-effective methods of joining or repairing Ti-clad steel plates.

Conclusions

• The interlayer-Ti interface and first Ti layer show the highest hardness levels in most of the different welded joints. The maximum hardnesses in the welded joints made with the Ni-Ti, NiCu-Ti, and NiCr-Ti interlayers were 607, 568, and 554 $HV_{0.5}$, respectively. Some degree of softening was induced in the Ni-Ti welded joint by the thermal cycles of additional Ti layers. The PWHT did not induce a major softening in the weld metal deposited in these three welded joints.

• In the V-Ti and Ti-V systems, the maximum hardnesses of the weld deposits at the Fe-V interface were 307 and 409 $HV_{0.5}$, respectively; however, the presence of microcracking at that interface may have affected the hardness reading obtained from the V-Ti interlayer weld deposit.

• The maximum hardnesses observed in the welded joints made with the Cu-Ti interlayer ranged from 300–350 $HV_{0.5}$. The high hardness region observed in the welded joints made with a combination of CSC-GMAW and GTAW-P processes was wider than the region observed in the welded joint made with the CSC-GMAW process only. As a result of PWHT, the hardness level through the weld deposit dropped to approximately 200 $HV_{0.5}$.

• Most of the samples obtained from the welded joints in the as-welded and PWHTed conditions failed the side bend test. The samples from the Ni-Ti, NiCu-Ti, and NiCr-Ti welded joints failed along the interlayer-Ti interface and through the Ti weld deposits. In the samples obtained from the Cu-Ti/(CSC-GMAW + GTAW-P) welded joint, cracking was observed only along the Cu-Ti interface and in the first Ti layer. Most of the samples obtained from Cu-Ti/CSC-GMAW welded joint failed along Cu-Ti interface.

• A bend sample obtained from the Ti-V-Fe system passed the bend test in the PWHTed condition. The observed cracks were confined to the V interlayer and were shorter than ⅛ in. The effect of these microcracks on the integrity of the welded joint during service is not yet known.

• The shear-bond strength samples representing the Fe-Cu and the Cu-Ti interfaces of the welded joints made with the Cu-Ti interlayer and with a combination of CSC-GMAW and GTAW-P processes passed the test in the as-welded, PWHT, and thermal-cycled conditions. The shear-bond strength of these interfaces ranges between 204.4 and 259.8 MPa (29.6 and 37.6 ksi) and was higher than the 137.9 MPa (20.0 ksi) shear-bond strength required for reactive and refractory metal clad plate by ASTM standards. The Fe-Cu interface showed a more ductile behavior than that of the Cu-Ti interface.

Acknowledgments

This paper was prepared based on development work supported by DMC Clad Metal, Materials Technology Institute, and Eastman Chemical, as part of a group-sponsored project at EWI, Columbus, Ohio.

References

1. Banker, J. G. 1996. Titanium-steel explosion clad. Stainless Steel World, (6): 65–69.

2. Hardwick, R. 2001. Advances leading to the new clads on the future. *Stainless Steel World*, pp. 149–154.

3. Banker, J. G. 1993. Bonded Titanium/Steel Components, U.S. Patent 5,190,831.

4. Murayama, J., and Komizo, Y. 1991. Titanium-Clad Steel and a Method for the Manufacture Thereof, European Patent 0 238 854 B1.

5. Hardwick, R. 1993. Method for Producing Clad Metal Plate, European Patent 0 535 817 A2.

6. Suenaga, H., Ishikawa, M., and Ninakawa, K. 1993. Method for Manufacturing Titanium Clad Steel Plate, European Patent 0 406 688 B1 (Mar. 1993).

7. Kawanami, T., Shirasuna, S., Shirogane, S., and Segawa, A. 1992. An investigation of the characteristic of bonding strength in titanium clad steel. *Titanium '92 Science and Technology*, Vol. II, Proceedings of a symposium sponsored by the titanium committee on Minerals, Metals and Materials, Structural Metals Division, held at Seventh World Titanium Conference, San Diego, Calif., edited by F. H. Froes and I. L. Caplan, pp. 1609–1617.

8. Pin´kovskii, I. V., et al. 1988. Special features of resistance welding VT1-0 titanium to low carbon steel. *Welding International* (3): 241, 242.

9. Bellini, L., and Giumelli, R. 1987. Welding of titanium clad components. *Welding International* (2): 155–164.

10. Pocalyko, A. 1987. Fabrication of explosion-welded titanium-clad composites. *Welding Journal* 66(1): 24–30.

11. Titanium, Zirconium, and Tantalum Clad Steel Construction.

12. Ramirez, J. E. Characterization of CSC-GMAW Ti-rich weld overlays. Approved for publication in the *Welding Journal*.

13. Huismann, G. 2001. Energy based synergistic MIG control system, IIW Doc. 212-1000-01.

14. Huismann, G. 1999. Introduction of a new MIG process: Advantages and possibilities. IIW DOC. 212-952-99.

15. Huismann, G. 2000. Direct control of the material transfer: The controlled short circuiting (CSC)-MIG process. *Proceedings on GMA for the 21th Century,* pp. 165–172, Orlando, Fla.

16. Huismann, G. 2002. Energy based synergistic pulsed MIG control system. *Proceedings on Trends in Welding Research*, Pine Mountain, Ga.

17. Huismann, G. 2001. Advantages in using the stick out for increasing the burn off rate in gas metal arc welding. *7th International Symposium of Japan Welding Society,* Kobe, Japan.

18. Ramirez, J. E. Development of joining technology for Ti-clad steel plates. Sent to *Welding Journal* for review.

19. ASTM B898: *Standard Specification for Reactive and Refractory Metal Clad Plate*.